CrossMark

ORIGINAL PAPER

Widespread tau seeding activity at early Braak stages

Jennifer L. Furman[5] · Jaime Vaquer-Alicea[5] · Charles L. White III[2] ·
Nigel J. Cairns[3] · Peter T. Nelson[4] · Marc I. Diamond[1]

Abstract Transcellular propagation of tau aggregates may underlie the progression of pathology in Alzheimer's disease (AD) and other tauopathies. Braak staging (B1, B2, B3) is based on phospho-tau accumulation within connected brain regions: entorhinal cortex (B1); hippocampus/limbic system (B2); and frontal and parietal lobes (B3). We previously developed a specific and sensitive assay that uses flow cytometry to quantify tissue seeding activity based on fluorescence resonance energy transfer (FRET) in cells that stably express tau reporter proteins. In a tauopathy mouse model, we have detected seeding activity far in advance of histopathological changes. It remains unknown whether individuals with AD also develop seeding activity prior to accumulation of phospho-tau. We measured tau seeding activity across four brain regions (hippocampus, frontal lobe, parietal lobe, and cerebellum) in 104 fresh-frozen human AD brain samples from all Braak stages. We observed widespread seeding activity, notably in regions predicted to be free of phospho-tau deposition, and in detergent-insoluble fractions that lacked tau detectable by ELISA. Seeding activity correlated positively with Braak stage and negatively with MMSE. Our results are consistent with early transcellular propagation of tau seeds that triggers subsequent development of neuropathology. The FRET-based seeding assay may also complement standard neuropathological classification of tauopathies.

Keywords Tau · Seeding · Alzheimer's disease · Braak staging · Neuropathology · Propagation

✉ Marc I. Diamond
  marc.diamond@utsouthwestern.edu

1 Center for Alzheimer's and Neurodegenerative Diseases, University of Texas Southwestern Medical Center, 5323 Harry Hines Blvd., NL10.120, Dallas, TX 75390, USA

2 Department of Pathology, Southwestern Medical Center, University of Texas Southwestern Medical Center, Dallas, TX, USA

3 Department of Neurology, Washington University, St. Louis, MO, USA

4 Department of Pathology, Sanders-Brown Center on Aging, University of Kentucky, Lexington, KY, USA

5 Center for Alzheimer's and Neurodegenerative Diseases, University of Texas Southwestern Medical Center, Dallas, TX 75390, USA

Introduction

Alzheimer's disease (AD) is characterized by learning and memory deficits and brain deposition of extracellular amyloid beta plaques and intracellular neurofibrillary tangles. In comparison to amyloid beta plaque load, tau accumulation better correlates with cognitive disturbances [3, 17, 27, 34], suggesting a fundamental role in neurodegeneration. The precise toxic form(s) of tau is unknown, but evidence suggests that transcellular propagation of tau aggregates, or, seeds, could underlie disease progression [11, 12, 15, 18, 24, 28, 36]. Indeed, we and others have found that tau has essential prion properties [10, 11, 30]. The prion model predicts that tau seeds escape one neuron, are internalized by another, and serve as a template to convert native tau monomer into an ordered assembly [8, 11, 14, 19, 23, 30]. In prior work, we have hypothesized that transcellular propagation of tau seeding activity underlies the pattern of neuropathology in tauopathies such as AD [15, 31].

Tau pathology in AD develops progressively in synaptically connected brain regions. This forms the basis of Braak Staging [6, 7, 29, 33, 39], a well-established method that scores accumulation of phospho-tau based on AT8 antibody staining of specific brain regions [5]. While Braak staging has proved very useful, variance in staining and analysis adds a subjective aspect to the diagnosis of AD and other tauopathies. Furthermore, these methods are bounded by the detection limits of immunohistochemistry, while more sensitive methods could highlight earlier or more widespread abnormalities.

To quantify tau seeding activity, we previously developed a cellular biosensor assay [20]. This is based on stable expression of tau repeat domain (RD) containing a single disease-associated mutation (P301S) that is fused to cyan or yellow fluorescent protein (CFP or YFP). Exogenous tau aggregate seeds delivered to the cell interior with cationic lipids (Lipofectamine 2000) trigger aggregation of intracellular RD-CFP/YFP by acting as a conformational template. The close approximation of CFP and YFP within an aggregate results in fluorescence resonance energy transfer (FRET) that is quantified by flow cytometry. This enables determination of tau aggregate seed "titer" over 3 orders of magnitude. We have not observed cross-reactivity with other amyloid proteins in the seeding assay [20, 30], and immunodepletion with an anti-tau antibody eliminates seeding activity from samples [20, 37]. Thus, the assay appears highly sensitive and specific.

We have previously determined that aged, healthy human brains and tau knockout mice lack tau seeding activity [20]. By contrast, tau seeding activity progressively increases with age in the PS19 tauopathy mouse model (which expresses human 1N,4R tau containing the P301S mutation), and anticipates neuropathological changes (AT8, MC1, and thioflavin staining) by many months [20]. These results are consistent with the idea that tau seeding triggers subsequent development of neuropathology. However, it is unknown whether a similar process might occur in AD. To test this prediction, we have measured tau seeding activity in fresh-frozen human brain specimens from multiple brain regions, across all Braak stages. We correlated seeding activity with Braak stage, clinical parameters, and tau biochemistry.

Materials and methods

Cell culture

HEK 293T cells were grown in DMEM (Gibco) supplemented with 10% fetal bovine serum (Sigma-Aldrich), 1% penicillin/streptomycin (Gibco), and 1% GlutaMax (Gibco). Cells were cultured at 37 °C with 5% CO_2 in a humidified incubator.

Brain tissue

We analyzed fresh-frozen specimens from brains that were previously categorized by qualified neuropathologists (C.L.W., N.J.C., P.T.N.). 40 subjects were staged according to Braak criteria as B1, B2, or B3 (defined as Braak I–II, Braak III–IV, or Braak V–VI, respectively). Subjects were diagnosed using standard tau histological measures (described below) and the 2012 criteria specified by the National Institute on Aging and the Alzheimer's Association [5, 21]. Samples consisted of gray matter obtained from four distinct brain regions (hippocampus, frontal lobe (Brodmann Areas 8/9), parietal lobe (Brodmann Areas 39/40), or cerebellum) typically affected differentially with tau pathology through AD progression. Negative control tissue was obtained from individuals with psychiatric disturbance, or Huntington's disease. In total, 126 brain specimens were analyzed.

Sample preparation

Fresh-frozen brain tissues were suspended in TBS containing EDTA-free complete protease inhibitors (Roche) such that the total concentration was 10% w/vol. Samples were homogenized at 75 watts with pulsing using a probe sonicator (Omni International) for 15 min on ice in a hood. Between each sample, we washed the probe with three isopropanol and distilled water rinses to prevent cross-contamination. Lysates were centrifuged at 23,000×g for 15 min, and the supernatant was retained (total fraction). Protein concentration was measured with BCA (Pierce) and normalized between all samples at 2 μg/μl. Fractions were aliquoted and stored at −80 °C until further use to avoid multiple freeze/thaw cycles.

Biochemical extraction

Biochemical extraction was performed as described previously [9]. Total fractions (described above) were centrifuged at 100,000×g for 60 min at 4 °C, and the supernatant was collected (soluble fraction). Pellets were resuspended in 1% sarkosyl, incubated for 30 min at room temperature with shaking, and centrifuged again at 100,000×g for 60 min at 4 °C. The resultant pellet was resuspended in TBS (insoluble fraction). Soluble and insoluble tau fractions were standardized by volume for ELISA and seeding assays.

Tau ELISA

A total tau "sandwich" ELISA was performed as described previously [1]. All antibodies were kindly provided by Dr. Peter Davies (Albert Einstein College of Medicine). 96-well round-bottom plates (Corning) were coated for 48 h at 4 °C

with DA-31 (aa 150–190) diluted in sodium bicarbonate buffer (6 µg/mL). Plates were rinsed with PBS three times, blocked for 2 h at room temperature with Starting Block (Pierce), and rinsed with PBS five additional times. Total (1 µL), soluble (1 µL), and insoluble (0.3 µL) fractions were diluted in SuperBlock solution (Pierce; 20% SuperBlock, diluted in TBS), and 50 µL sample was added per well. DA-9 (aa 102–150) was conjugated to HRP using the Lighting-Link HRP Conjugation Kit (Innova Biosciences), diluted 1:50 in SuperBlock solution, and 50 µL was added per well (15 µg/mL). Sample + detection antibody complexes were incubated overnight at 4 °C. Plates were washed with PBS nine times with a 15-s incubation between each wash, and 75 µL 1-Step Ultra TMB Substrate Solution (Pierce) was added. Plates were developed for 30 min, and the reaction was quenched with 2 M sulfuric acid. Absorbance was measured at 450 nm using an Epoch plate reader (BioTek). Each plate contained a standard curve, and all samples were run in triplicate.

Biochemical quantification

Tau concentration was calculated using GraphPad Prism software. Standard curves were made using 2N,4R recombinant protein (rPeptide) ranging from 15.6 to 1000 pg/mL and were fitted using the sigmoidal, 4PL, $X = \log(\text{concentration})$ nonlinear regression model. Samples were diluted so that concentrations fell on the linear portion of the standard curve.

Tau seeding

Tau seeding activity was quantified as detailed previously [16, 20]. HEK 293T cells stably expressing the aggregation-prone repeat domain (RD) of tau containing the disease-associated P301S mutation tagged to either CFP or YFP were transduced with human brain homogenates. At 60–65% confluency, transduction complexes consisting of lysate (either 20 µg total, 2 µl soluble, or 5 µl insoluble fraction), Opti-MEM (Gibco), and Lipofectamine 2000 (Invitrogen) were added to cells. Following treatment, cells were incubated for 24 h prior to harvesting for FRET flow cytometry. Prior to FRET flow cytometry, we always confirmed visible RD-CFP/YFP inclusions in positive wells. Standardized seeding activity, reported here, is a fold change over background level of biosensor cells treated with empty liposomes, which is arbitrarily set at 1% positivity in the FRET gate.

FRET flow cytometry

FRET flow cytometry was performed as described previously [16, 20]. Following 24 h treatment, cells were trypsinized, centrifuged, and fixed in 2% paraformaldehyde (Electron Microscopy Sciences). Cells were resuspended in flow cytometry buffer (HBSS, PBS, 1% FBS, and 1 mM EDTA) and analyzed using the MACSQuant VYB flow cytometer (Miltenyi Biotec). CFP, YFP, and FRET signals were detected with the following settings: CFP (405 laser; 450/50 filter), YFP (488 laser; 525/50 filter), FRET (405 laser; 525/50 filter). Samples were run in quadruplicate, and 15,000–20,000 singlets were captured per well.

Immunodepletion

Total fractions were sonicated in pulse mode (30 sec on, 60 sec off) for 2 h using a Q700 Sonicator (QSonica) at a power of 100–110 watts (amplitude 50) to ensure that very large, insoluble aggregates were dissociated. Lysate was then incubated with control agarose beads to eliminate nonspecific binding, then with Protein A/G Agarose beads (Santa Cruz) coated with either AT8 (Thermo Fisher Scientific) or control IgG (BioLegend) antibody. Following a 2 h incubation, samples were centrifuged at 1000 x g for 3 min. Supernatant was preserved. Beads were washed 4 times with Ag/Ab gentle binding buffer, and bound antigen was eluted with low pH elution buffer. Supernatant was re-applied to antibody-bound beads, and the incubation-centrifugation-wash-elution steps were repeated a total of 3 times for maximal immunodepletion. After the final incubation, flow-through was preserved for seeding experiments.

Flow cytometry analysis

FlowJo v10 software was used for analysis. Gating strategy was similar to that described previously [16, 20]. CFP and YFP spillover into the FRET channel were excluded using compensation and the "False FRET" gate. Empty liposome-treated cells were used as the baseline for background seeding, and FRET-positive events were identified from a FRET vs. CFP bivariate plot. The median fluorescence intensity (MFI) of FRET-positive events was recorded. Integrated FRET Density (IFD; the product of percent cells FRET-positive and MFI) is presented here. This integrates the amount of seeding per population of cells with the degree of seeding within a positive cell.

Confocal microscopy

All cells were grown and treated on microslides (Ibidi). Cells were fixed with 4% paraformaldehyde, and confocal images were obtained with a Zeiss LSM 780 Inverted confocal/multiphoton microscope.

Heat map

Heat maps were generated using MATLAB software (MathWorks). The Integrated FRET Density values were

log-transformed and colored on a blue scale. Values less than 1.5-fold above untreated controls (non-significant levels) are shaded with light blue. The remaining values are shaded from light to dark blue on a continuum, with the latter representing the highest fold increase in IFD. If no sample was available, the rectangle is filled with gray dots.

Immunohistochemistry

Paraffin sections were cut at 4-μm thickness on a rotary microtome, mounted on positively charged glass slides, and air-dried overnight. Sections were deparaffinized in xylene and alcohol, pretreated in 98% formic acid for 5 min at room temperature, and rinsed in water. Immunostaining was performed at room temperature on a Bond III automated immunostainer (Leica Biosystems Inc) using phospho-tau monoclonal antibody AT8 (Pierce Biotechnology; 1:200 for 30 min) and the Bond Polymer Refine detection system, which includes H_2O_2 block, EDTA-based epitope retrieval solution, rabbit anti-mouse IgG secondary antibody, anti-rabbit poly-HRP-IgG, DAB, and hematoxylin counterstain. Sections were dehydrated in a graded series of ethanol dilutions and xylene, mounted on coverslips, and reviewed on a Ni-U light microscope (Nikon Instruments Inc.). For preparation of photomicrographs, slides were imaged on an Aperio ScanScope CS whole slide imager (Leica) using a 20× objective, and selected fields captured using Aperio ImageScope v12 software.

Statistics

For all seeding experiments, cells treated with empty liposomes served as the control group. We used a two-tailed

t test and set significance at $p < 0.01$. For correlational analyses, we performed nonparametric Spearman rank-order tests. r values represent the correlation between seeding in each brain region and age, MMSE, or Braak stage, with significance set at $p < 0.05$.

Results

Tau seeding detected across brain regions and Braak stages

Braak staging requires detection of phospho-tau pathology in discrete brain regions. To test for a relationship of Braak staging and tau seeding activity, we used the FRET flow cytometry assay to quantify seeding activity in homogenates prepared from fresh-frozen brain specimens from all Braak stages, across four regions (hippocampus, frontal and parietal lobes, and cerebellum). We analyzed tissue from 40 individuals previously staged as B1, B2, or B3 based on standard histopathological criteria (Supplemental Figure 1) and 7 additional individuals not reported to harbor tau pathology. Where possible, we analyzed multiple brain regions from the same subject.

All negative samples lacked seeding activity in each brain region (Fig. 1a–d). Most B1 samples exhibited tau seeding activity in the hippocampus, but not in other regions (Fig. 1a–d). B2 samples all exhibited hippocampal tau seeding (Fig. 1a), and B3 samples uniformly scored positive in hippocampus, frontal, and parietal lobes (Fig. 1b, c). In many instances, we observed seeding activity in brain regions that usually lack tau pathology, as monitored by histology. For example, most B1
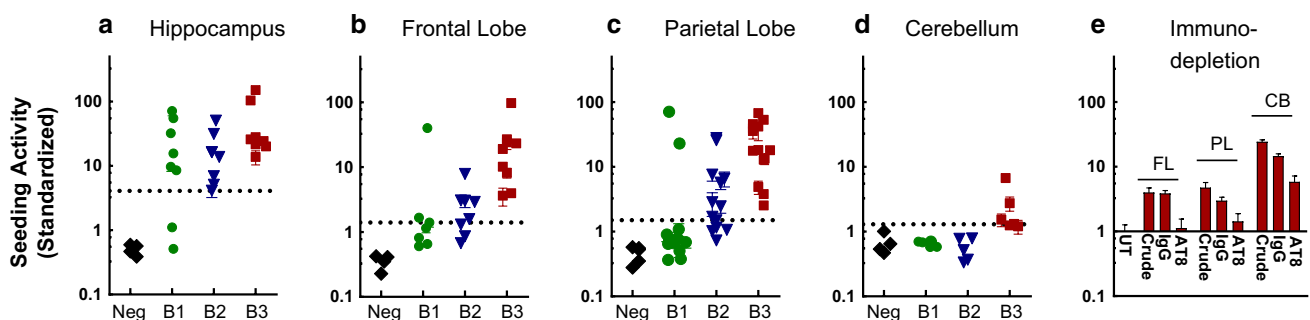

Fig. 1 Tau seeding activity is present in multiple brain regions and increases with Braak stage. 20 µg of clarified human brain lysate was transduced into Tau-RD-P301S CFP/YFP biosensor cells, which were harvested for FRET flow cytometry after 24 h. Hippocampus (**a**), frontal lobe (**b**), and parietal lobe (**c**) all consistently scored positive for seeding from B3 brains (represented by *red squares*). B2 brains (represented by *blue triangles*) also demonstrated strong hippocampal seeding activity and moderate cortical seeding. B1 subjects (represented by *green circles*) consistently showed hippocampal seeding

activity. Cerebellum (**d**) contained seeding activity in a few B3 samples. *Error bars* denote SEM, and *dashed lines* represent threshold for significant seeding ($p < 0.01$), as compared to cells treated with empty liposomes. Standardized seeding activity represents the fold change in signal over negative control biosensor cells. Immunodepletion (**e**) with AT8 antibody, but not control IgG, strongly reduced seeding in frontal and parietal lobes, and partially from cerebellum. Data represent 4 replicates from a single patient; error bars denote SEM
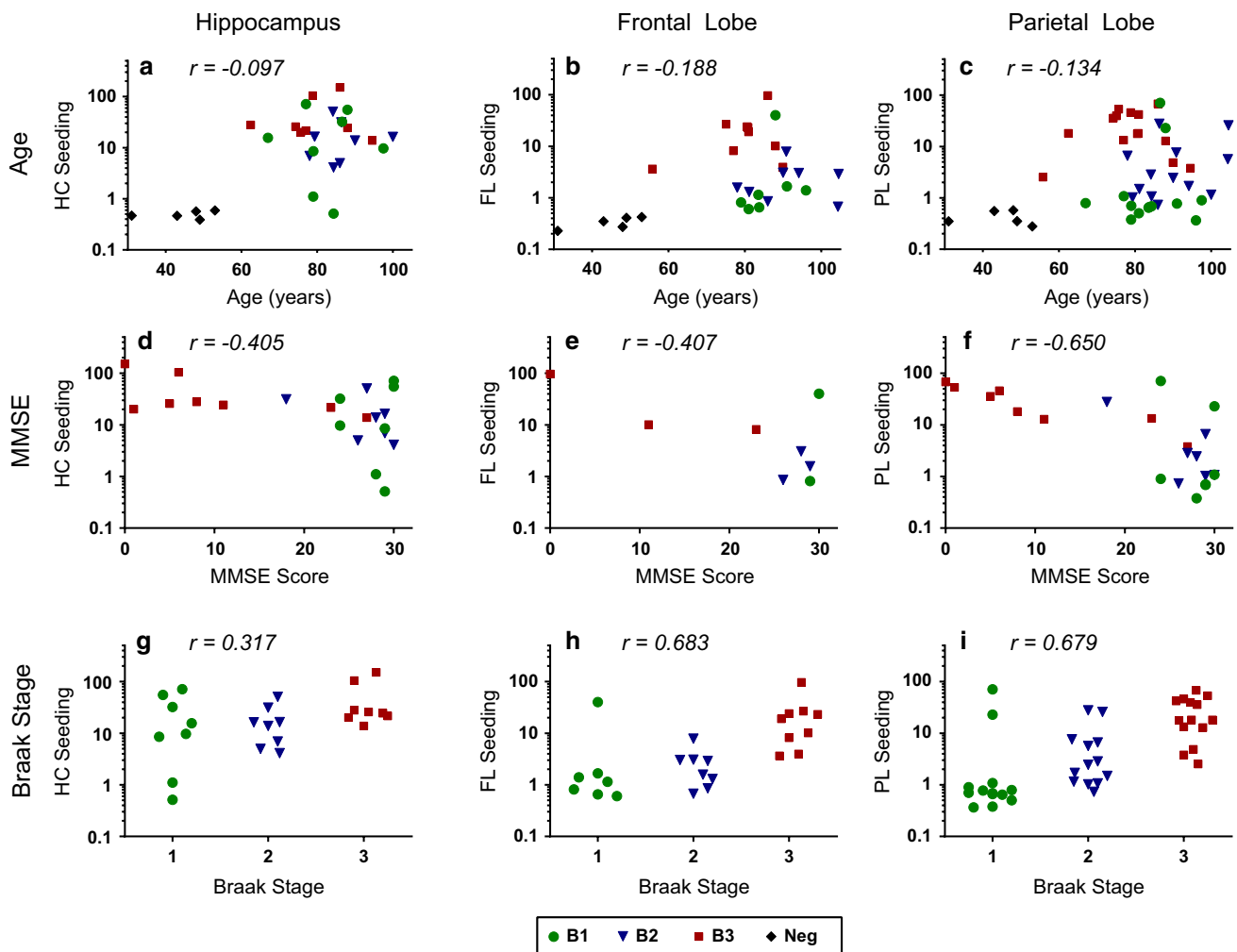
Fig. 2 Correlation of tau seeding with MMSE and Braak stage. We evaluated seeding activity with subject age (**a–c**), MMSE (**d–f**) and Braak stage (**g–i**) using nonparametric Spearman correlational analyses. Age and seeding activity did not correlate; MMSE and seeding activity negatively correlated; and Braak stage and seeding activity positively correlated ($p < 0.05$)

samples, in which tau pathology is generally limited to entorhinal cortex, had seeding activity in the hippocampus (Fig. 1a) and often in cortical regions (Fig. 1b, c). B2 samples, in which pathology is generally restricted to limbic regions, frequently exhibited seeding activity in frontal and parietal lobes (Fig. 1b, c). Finally, in B3 cases we even observed seeding in cerebellum, despite the fact that this region does not typically exhibit tau pathology (Fig. 1d). To ensure that seeding activity was specific to tau, we performed immunodepletion experiments on a subset of samples. Following incubation with either a negative control antibody (IgG) or an anti-tau antibody (AT8), we consistently observed a significant reduction in seeding activity when lysate was immunodepleted with AT8, but not IgG (Fig. 1e). Cerebellar seeding activity was depleted less efficiently. Possibilities for this are discussed below.

Seeding activity correlates with lower MMSE score and higher Braak stage

We next tested for correlation of seeding activity with other clinical and pathologic characteristics. Age did not correlate with seeding activity in any brain region (Fig. 2a–c). Seeding activity and cognitive status [as measured by the Mini-Mental State Examination (MMSE)] negatively correlated (Fig. 2d–f), particularly in the parietal lobe. Seeding activity correlated highly with Braak stage (Fig. 2g–i) in frontal and parietal lobes.

Seeding activity by region within individual brains

Braak and Braak first reported progressive and stereotypical neurofibrillary tangle (NFT) accumulation in AD brains over two decades ago [6, 7]. In recent years,
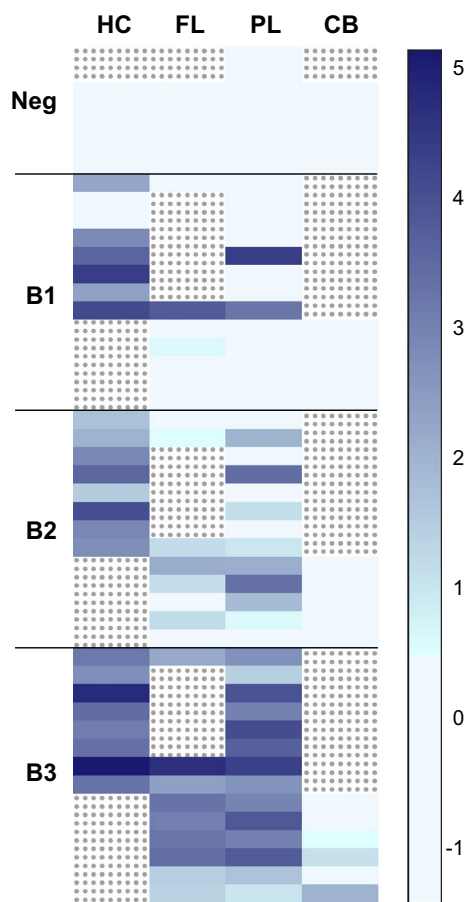
Fig. 3 Seeding activity determined by region in individuals. Relative tau seeding activity was assessed in brain regions within the same individuals. *Each row* represents an individual subject (*n* = 47), and *each column* represents a specific brain region. Samples not provided for a region are colored with *gray dots*. Representative seeding values are *shaded light* to *dark blue* with the latter corresponding to highest seeding activity. Seeding activity is highest in hippocampus and increases with Braak stage

numerous mouse studies have demonstrated that tau aggregates inoculated into the brain trigger spreading tau pathology [2, 11, 12, 22, 24, 26, 30, 35]. Further, we previously observed a steady increase in tau seeding activity in the PS19 tauopathy mouse brain, even in the absence of seed inoculation [20, 38]. However, it is unknown how seeding activity might vary across brain regions at different Braak stages within individuals. Thus, we charted the previous seeding data with a heat map, organized by individual. Tissue from all four brain regions was not available for any one subject (denoted by boxes with gray dots), although for every individual at least two brain regions were provided. For nearly every brain in which seeding was detectable, we observed the highest seeding in hippocampus, next highest in neocortex, and lowest in cerebellum (Fig. 3). Additionally, most cases contained higher seeding activity in frontal rather than parietal lobes,

consistent with the original pathological characterization by Braak and Braak [6].

Seeding detects pathology more sensitively than biochemistry

Accumulation of detergent-insoluble tau is associated with progressive pathology. Thus, we tested the relative sensitivity of solubility analysis of tau vs. its seeding activity. We extracted total, soluble, and sarkosyl-insoluble fractions from each brain sample and measured tau levels using an ultra-sensitive ELISA developed by the Peter Davies laboratory [1]. We detected tau in all total (Fig. 4a) and soluble (Fig. 4b) fractions, regardless of brain region or Braak stage, whereas we observed a more variable presence of detergent-insoluble tau (Fig. 4c), which correlated with the reported Braak stage: minimal in B1, moderate in B2, and extensive in B3, excluding cerebellum, which lacked insoluble tau as measured by ELISA.

We then analyzed each biochemical fraction for seeding activity. We observed seeding in many total (Fig. 4d), soluble (Fig. 4e), and insoluble (Fig. 4f) fractions with the exception of negative control subjects, but no correlation with tau levels. Importantly, a large number of B1, B2, or B3 samples had no apparent insoluble tau as characterized by ELISA, yet they exhibited strong seeding activity (Fig. 4f, highlighted in yellow). Overall, we detected seeding activity in 82 of 104 insoluble sample fractions. Of note, 18 of these 82 (~22%) initially scored negative when seeding was first evaluated from the total fraction. This indicates that when the total lysate scores negative it is still possible to enrich seeding activity using detergent fractionation. In no instance did we detect seeding in the total fraction but not the insoluble fraction. We conclude that tau seeding activity does not correlate with total tau protein level, and that the FRET seeding assay is highly sensitive for the detection of tau aggregate seeds.

Discussion

Tau pathology in AD develops progressively in regions of the brain with known synaptic connectivity, and prion-like transcellular propagation of seeds has been proposed to explain this observation [4, 10, 20, 30]. This model makes a strong prediction that seeding activity should anticipate subsequent development of neuropathology. To test this idea, we quantified tau seeding activity in fresh-frozen brain samples derived from 40 individuals at different Braak stages, across four brain regions. We detected proteopathic tau seeding activity across specimens more extensively than is typically observed by histopathology or biochemical studies alone. In particular, we observed
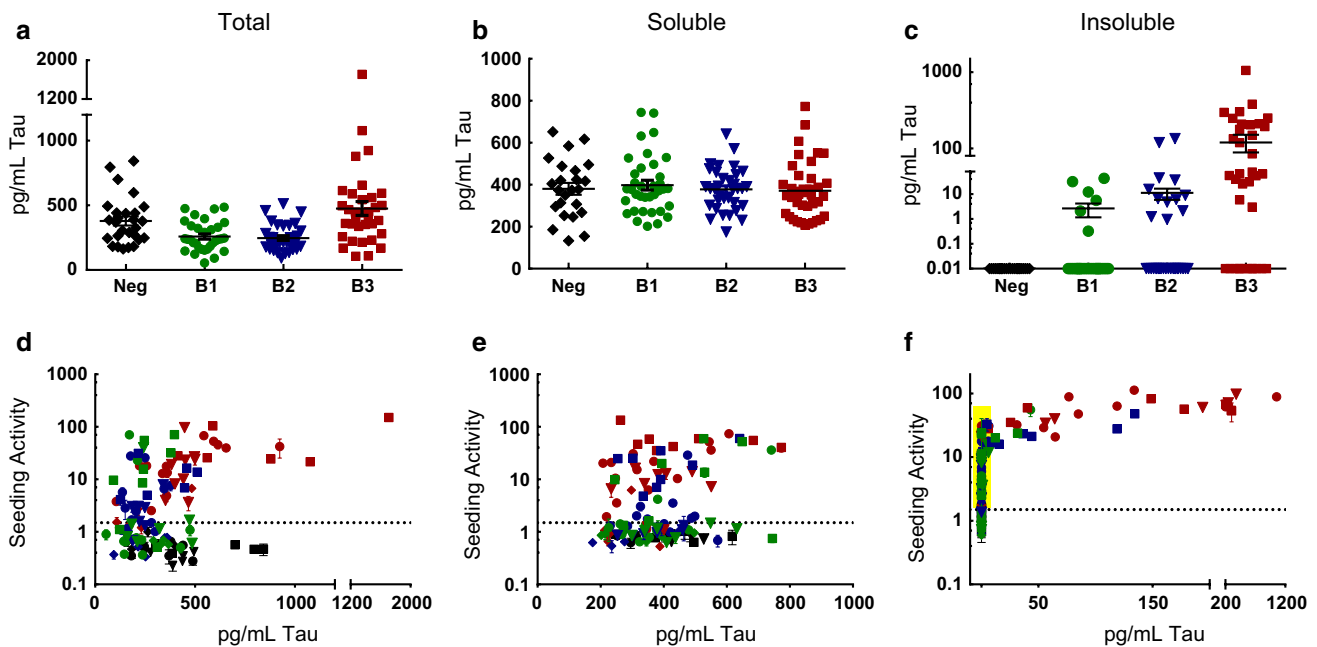
Fig. 4 Biochemical characterization of brain homogenates. Brain lysates were biochemically extracted, and subsequent fractions were quantified using ELISA (**a–c**) and FRET flow cytometry (**d–f**). All samples contained total (**a, d**) and soluble (**b, e**) tau. Insoluble tau (**c, f**) was measurable in only a subset of samples. Seeding activity was present variably in total (**d**) or soluble (**e**) fractions, and was present in the majority of insoluble fractions (**f**), even those that did not score positive with ELISA, or were from early Braak stages. The *yellow box* (**f**) highlights 41 samples that were ELISA-negative yet seed-positive

robust seeding activity in many hippocampal samples from B1 brains and in many parietal and frontal lobe samples from B2 brains. In a subset of B3 brains, we even observed seeding activity within the cerebellum, which typically has no detectable tau pathology based on immunohistochemistry. Importantly, despite trying several anti-tau antibodies in addition to AT8, together or in sequence, we never achieved full depletion of cerebellar tau seeding activity. Although we have never observed cross-seeding events between other amyloids and tau, we conclude that some seeding activity in the cerebellum might represent a non-tau factor, or tau species for which the epitopes are masked due to post-translational modifications, protein interactions, or distinct strain structure. Taken together, however, our findings support the model of transcellular propagation of tau pathology, and suggest that seed detection might augment standard histopathological analysis.

Seed detection as a quantitative adjunct for neuropathology

Pathological assessment of NFTs was first described by Braak and Braak several decades ago [6, 7], and their AT8 staining protocols are now the gold standard for pathological characterization of AD. Although staining methods are well established and the progression of phospho-tau pathology is predictable, the analysis of a brain still requires the subjective impression of a qualified neuropathologist. While the recently revised grouping of Braak stages described by the National Institute on Aging and the Alzheimer's Association [21] may help to standardize diagnosis, Braak staging by immunohistochemistry remains an imperfect metric of tau pathology.

The FRET flow cytometry assay we have previously described sensitively quantifies tau seeding activity in biological samples [16, 20]. We have never observed non-specific seeding of tau by heterologous fibrillar species, suggesting that it is also specific [20, 30]. The assay is user-friendly and relatively high throughput, with a continuous signal spectrum. It requires appropriate positive and negative controls, along with a dedicated flow cytometer and an experienced operator, which may limit its broad applicability.

With this assay we detected tau seeding activity in human lysates across multiple brain regions and Braak stages. Seeding activity correlates with Braak staging, but appears to be more sensitive to the presence of pathological tau. This suggests that the seeding assay could complement standard histopathology. Quantification of seeding activity in multiple regions or sub-regions of brain might reveal new aspects of tauopathy that cannot be visualized by immunohistochemistry or biochemistry, especially early in disease.

The tau seeding assay requires relatively small amounts of brain tissue (<100 μg), which may be beneficial when samples are limited. In this study, we used fresh-frozen tissue,

which precluded simultaneous analysis of the same brain region by histopathology. However, future work will determine the feasibility of using fixed tissue, which we expect will be compatible given the resistance of amyloid beta and alpha synuclein seeds to formaldehyde fixation [13, 32]. If compatible with the tau seeding assay, fixed tissue analysis could open up important possibilities in combination with neuropathological analysis of the same region. While evaluation of seeding activity in one small sample may not accurately represent the entire brain structure, its relatively high throughput nature enables multiple samples to be tested across brain regions without much additional labor. In combination with current AT8 staining protocols, we anticipate that the two metrics together might augment the detection, quantification, and characterization of tau pathology.

Seeding as an early marker of pathology

We observed that seeding activity generally correlates with the characteristic phospho-tau staining patterns described by Braak staging. However, numerous tissue samples exhibited obvious seeding activity prior to when Braak staging would predict tau pathology. For example, according to B1 staging guidelines, phospho-tau is restricted to entorhinal cortex, yet we observed seeding activity in >50% of B1 hippocampal homogenates. Similarly, in B2 brains, where tau pathology is limited to the entorhinal or limbic systems, we consistently measured tau seeding activity in parietal and frontal lobes. In B3 brains, we observed seeding activity in every hippocampal and cortical sample tested, and even in occasional cerebellar samples, which typically lack phospho-tau histopathology. Immunodepletion studies along with previously published material [30] suggest that the seeding activity quantified here is tau-specific and not the result of cross-seeding from another pathological source. In addition to standard histological patterns of tau pathology, seeding activity also proved to be more sensitive than standard biochemical analysis of tau in brain lysates. In numerous cases samples had no detectable insoluble tau based on an ultra-sensitive ELISA (detection level of ~24 pg/mL tau [1]), but scored positive with the FRET flow cytometry assay. Thus, we anticipate that the seeding assay might also augment standard biochemical analyses of insoluble (i.e., pathological) tau.

We previously observed that seeding activity is the earliest marker of disease in the PS19 tauopathy mouse model, as it appears months before multiple immunohistochemical markers score positive, including AT8, PG5, and MC1 [20]. Because the current work did not evaluate human tissue specimens in parallel for histopathology and seeding, as was done in the mouse study, we cannot conclude with certainty that seeding activity precedes deposition of phospho-tau in these human brain specimens. This must await simultaneous comparison with both methods of very closely spaced subregions of brain. Seeding activity that is detected prior to histopathological abnormality could be due to the presence of very small tau assemblies that are seed-competent (trimer or above [25]), but that may not feature abundant phosphorylation. Alternatively, the seeding species may be below the threshold of detection of any type of immunohistochemistry. Regardless, we hope future work will be able to determine the significance of seeding activity observed in the absence of histopathological tau abnormalities.

Tau seeding and the prion hypothesis

There is no evidence of inadvertent transmission of tau pathology between individuals. Nonetheless, in experimental systems, we and others have observed that tau acts as a prion in many other respects [10, 11, 30]. It is impossible to know whether trans-cellular propagation underlies progression of disease in patients until we have an effective therapy designed to block this process. However, the hypothesis that proteopathic seeds cause pathology clearly predicts that seeding activity should develop prior to the occurrence of neuropathology that is visible by stains for macromolecular protein assemblies. While this study has a critical limitation in that the fresh-frozen tissues studied with the FRET assay are not the same as those that were used for Braak staging of brains, the early and widespread detection of seeding is consistent with the prion model to explain progressive accumulation of tau pathology and neurological dysfunction in AD. We hope that future studies that employ a similar multimodal assessment of human tissues will clarify these initial observations.

References

1. Acker CM, Forest SK, Zinkowski R, Davies P, d'Abramo C (2013) Sensitive quantitative assays for tau and phospho-tau in transgenic mouse models. Neurobiol Aging 34:338–350. doi:10.1016/j.neurobiolaging.2012.05.010

2. Ahmed Z, Cooper J, Murray TK, Garn K, McNaughton E, Clarke H, Parhizkar S, Ward MA, Cavallini A, Jackson S et al (2014) A novel in vivo model of tau propagation with rapid and progressive neurofibrillary tangle pathology: the pattern of spread is determined by connectivity, not proximity. Acta Neuropathol 127:667–683. doi:10.1007/s00401-014-1254-6

3. Arriagada PV, Growdon JH, Hedley-Whyte ET, Hyman BT (1992) Neurofibrillary tangles but not senile plaques parallel duration and severity of Alzheimer's disease. Neurology 42:631–639

4. Boluda S, Iba M, Zhang B, Raible KM, Lee VM, Trojanowski JQ (2015) Differential induction and spread of tau pathology in young PS19 tau transgenic mice following intracerebral injections of pathological tau from Alzheimer's disease or corticobasal degeneration brains. Acta Neuropathol 129:221–237. doi:10.1007/s00401-014-1373-0

5. Braak H, Alafuzoff I, Arzberger T, Kretzschmar H, Del Tredici K (2006) Staging of Alzheimer disease-associated neurofibrillary pathology using paraffin sections and immunocytochemistry. Acta Neuropathol 112:389–404. doi:10.1007/s00401-006-0127-z

6. Braak H, Braak E (1991) Neuropathological stageing of Alzheimer-related changes. Acta Neuropathol 82:239–259

7. Braak H, Braak E (1995) Staging of Alzheimer's disease-related neurofibrillary changes. Neurobiol Aging 16:271–278 **(discussion 278–284)**

8. Calafate S, Buist A, Miskiewicz K, Vijayan V, Daneels G, de Strooper B, de Wit J, Verstreken P, Moechars D (2015) Synaptic contacts enhance cell-to-cell tau pathology propagation. Cell Rep 11:1176–1183. doi:10.1016/j.celrep.2015.04.043

9. Chai X, Wu S, Murray TK, Kinley R, Cella CV, Sims H, Buckner N, Hanmer J, Davies P, O'Neill MJ et al (2011) Passive immunization with anti-tau antibodies in two transgenic models: reduction of tau pathology and delay of disease progression. J Biol Chem 286:34457–34467. doi:10.1074/jbc.M111.229633

10. Clavaguera F, Akatsu H, Fraser G, Crowther RA, Frank S, Hench J, Probst A, Winkler DT, Reichwald J, Staufenbiel M et al (2013) Brain homogenates from human tauopathies induce tau inclusions in mouse brain. Proc Natl Acad Sci USA 110:9535–9540. doi:10.1073/pnas.1301175110

11. Clavaguera F, Bolmont T, Crowther RA, Abramowski D, Frank S, Probst A, Fraser G, Stalder AK, Beibel M, Staufenbiel M et al (2009) Transmission and spreading of tauopathy in transgenic mouse brain. Nat Cell Biol 11:909–913. doi:10.1038/ncb1901

12. de Calignon A, Polydoro M, Suárez-Calvet M, William C, Adamowicz David H, Kopeikina Kathy J, Pitstick R, Sahara N, Ashe Karen H, Carlson George A et al (2012) Propagation of tau pathology in a model of early Alzheimer's disease. Neuron 73:685–697

13. Fritschi SK, Cintron A, Ye L, Mahler J, Buhler A, Baumann F, Neumann M, Nilsson KP, Hammarstrom P, Walker LC et al (2014) Abeta seeds resist inactivation by formaldehyde. Acta Neuropathol 128:477–484. doi:10.1007/s00401-014-1339-2

14. Frost B, Diamond MI (2009) Prion-like mechanisms in neurodegenerative diseases. Nat Rev Neurosci 11:155–159

15. Frost B, Jacks RL, Diamond MI (2009) Propagation of tau misfolding from the outside to the inside of a cell. J Biol Chem 284:12845–12852

16. Furman JL, Holmes BB, Diamond MI (2015) Sensitive detection of proteopathic seeding activity with FRET flow cytometry. J Vis Exp JoVE. doi:10.3791/53205

17. Grober E, Dickson D, Sliwinski MJ, Buschke H, Katz M, Crystal H, Lipton RB (1999) Memory and mental status correlates of modified Braak staging. Neurobiol Aging 20:573–579

18. Guo JL, Lee VMY (2011) Seeding of normal tau by pathological tau conformers drives pathogenesis of Alzheimer-like tangles. J Biol Chem. doi:10.1074/jbc.M110.209296

19. Holmes BB, DeVos SL, Kfoury N, Li M, Jacks R, Yanamandra K, Ouidja MO, Brodsky FM, Marasa J, Bagchi DP et al (2013) Heparan sulfate proteoglycans mediate internalization and propagation of specific proteopathic seeds. Proc Natl Acad Sci USA 110:E3138–E3147. doi:10.1073/pnas.1301440110

20. Holmes BB, Furman JL, Mahan TE, Yamasaki TR, Mirbaha H, Eades WC, Belaygorod L, Cairns NJ, Holtzman DM, Diamond MI (2014) Proteopathic tau seeding predicts tauopathy in vivo. Proc Natl Acad Sci USA. doi:10.1073/pnas.1411649111

21. Hyman BT, Phelps CH, Beach TG, Bigio EH, Cairns NJ, Carrillo MC, Dickson DW, Duyckaerts C, Frosch MP, Masliah E et al (2012) National Institute on Aging-Alzheimer's Association guidelines for the neuropathologic assessment of Alzheimer's disease. Alzheimers Dement 8:1–13. doi:10.1016/j.jalz.2011.10.007

22. Iba M, Guo JL, McBride JD, Zhang B, Trojanowski JQ, Lee VM (2013) Synthetic tau fibrils mediate transmission of neurofibrillary tangles in a transgenic mouse model of Alzheimer's-like tauopathy. J Neurosci 33:1024–1037. doi:10.1523/JNEUROSCI.2642-12.2013

23. Kfoury N, Holmes BB, Jiang H, Holtzman DM, Diamond MI (2012) Trans-cellular propagation of tau aggregation by fibrillar species. J Biol Chem 287:19440–19451. doi:10.1074/jbc.M112.346072

24. Liu L, Drouet V, Wu JW, Witter MP, Small SA, Clelland C, Duff K (2012) Trans-synaptic spread of tau pathology in vivo. PLoS One 7:e31302. doi:10.1371/journal.pone.0031302

25. Mirbaha H, Holmes BB, Sanders DW, Bieschke J, Diamond MI (2015) Tau trimers are the minimal propagation unit spontaneously internalized to seed intracellular aggregation. J Biol Chem 290:14893–14903. doi:10.1074/jbc.M115.652693

26. Peeraer E, Bottelbergs A, Van Kolen K, Stancu IC, Vasconcelos B, Mahieu M, Duytschaever H, Ver Donck L, Torremans A, Sluydts E et al (2015) Intracerebral injection of preformed synthetic tau fibrils initiates widespread tauopathy and neuronal loss in the brains of tau transgenic mice. Neurobiol Dis 73:83–95. doi:10.1016/j.nbd.2014.08.032

27. Polydoro M, Acker CM, Duff K, Castillo PE, Davies P (2009) Age-dependent impairment of cognitive and synaptic function in the htau mouse model of tau pathology. J Neurosci 29:10741–10749. doi:10.1523/JNEUROSCI.1065-09.2009

28. Prusiner SB (1984) Some speculations about prions, amyloid, and Alzheimer's disease. N Engl J Med 310:661–663. doi:10.1056/NEJM198403083101021

29. Raj A, Kuceyeski A, Weiner M (2012) A network diffusion model of disease progression in dementia. Neuron 73:1204–1215

30. Sanders DW, Kaufman SK, DeVos SL, Sharma AM, Mirbaha H, Li A, Barker SJ, Foley AC, Thorpe JR, Serpell LC et al (2014) Distinct tau prion strains propagate in cells and mice and define different tauopathies. Neuron. doi:10.1016/j.neuron.2014.04.047

31. Sanders DW, Kaufman SK, Holmes BB, Diamond MI (2016) Prions and protein assemblies that convey biological information in health and disease. Neuron 89:433–448. doi:10.1016/j.neuron.2016.01.026

32. Schweighauser M, Bacioglu M, Fritschi SK, Shimshek DR, Kahle PJ, Eisele YS, Jucker M (2015) Formaldehyde-fixed brain tissue from spontaneously ill alpha-synuclein transgenic mice induces fatal alpha-synucleinopathy in transgenic hosts. Acta Neuropathol 129:157–159. doi:10.1007/s00401-014-1360-5

33. Seeley WW, Crawford RK, Zhou J, Miller BL, Greicius MD (2009) Neurodegenerative diseases target large-scale human brain networks. Neuron 62:42–52. doi:10.1016/j.neuron.2009.03.024

34. Small SA, Duff K (2008) Linking Abeta and tau in late-onset Alzheimer's disease: a dual pathway hypothesis. Neuron 60:534–542. doi:10.1016/j.neuron.2008.11.007

35. Stancu IC, Vasconcelos B, Ris L, Wang P, Villers A, Peeraer E, Buist A, Terwel D, Baatsen P, Oyelami T et al (2015) Templated misfolding of tau by prion-like seeding along neuronal connections impairs neuronal network function and associated behavioral outcomes in tau transgenic mice. Acta Neuropathol 129:875–894. doi:10.1007/s00401-015-1413-4

36. Weaver CL, Espinoza M, Kress Y, Davies P (2000) Conformational change as one of the earliest alterations of tau in Alzheimer's disease. Neurobiol Aging 21:719–727

37. Yanamandra K, Kfoury N, Jiang H, Mahan TE, Ma S, Maloney SE, Wozniak DF, Diamond MI, Holtzman DM (2013) Anti-tau antibodies that block tau aggregate seeding in vitro markedly decrease pathology and improve cognition in vivo. Neuron 80:402–414. doi:10.1016/j.neuron.2013.07.046

38. Yoshiyama Y, Higuchi M, Zhang B, Huang SM, Iwata N, Saido TC, Maeda J, Suhara T, Trojanowski JQ, Lee VM (2007) Synapse loss and microglial activation precede tangles in a P301S tauopathy mouse model. Neuron 53:337–351. doi:10.1016/j.neuron.2007.01.010

39. Zhou J, Gennatas Efstathios D, Kramer Joel H, Miller Bruce L, Seeley William W (2012) Predicting regional neurodegeneration from the healthy brain functional connectome. Neuron 73:1216–1227